

See discussions, stats, and author profiles for this publication at: <https://www.researchgate.net/publication/273641386>

Effect of microhydration on the atmospherically important metastable carbonyl sulfide anion: Structure, energetic, and infrared study

ARTICLE *in* INTERNATIONAL JOURNAL OF QUANTUM CHEMISTRY · MARCH 2015

Impact Factor: 1.43 · DOI: 10.1002/qua.24902

READS

7

3 AUTHORS, INCLUDING:



Saptarsi Mondal

Indian Association for the Cultivation of Scie...

3 PUBLICATIONS 1 CITATION

SEE PROFILE

Effect of Microhydration on the Atmospherically Important Metastable Carbonyl Sulfide Anion: Structure, Energetic, and Infrared Study

Saptarsi Mondal, Avula Uday Teja, and Prashant Chandra Singh*

Structure, energetics, and vibrational frequency of the microhydrated carbonyl sulfide anion $[\text{OCS}^-(\text{H}_2\text{O})_n]$ ($n = 1-6$) have been explored by the systematic *ab initio* study to have a comprehensive understanding about the hydration-induced stabilization phenomenon of OCS^- . Water binds with the OCS^- in single hydrogen-bonded (SHB) or double hydrogen-bonded (DHB) fashion with $\text{O}-\text{H}\cdots\text{S}$ and $\text{O}-\text{H}\cdots\text{O}$ contacts. Maximum five water molecules can stay in a cyclic water network of these hydrated clusters forming interwater hydrogen bonding (IHB) with each other and out of this, maximum of two water molecules can bind directly to the OCS^- in (DHB)

arrangement. The stabilization energy values of $\text{OCS}^-(\text{H}_2\text{O})_n$ depict that ion-water interaction is significant up to four water molecules and beyond that OCS^- is stabilized by IHB between the water molecules. The CO stretching frequency of OCS^- gets red shifted, whereas CS stretching frequency gets blue shifted on hydration. Charge analysis of hydrated clusters of OCS^- indicates that negative charge moves toward oxygen from sulfur on hydration. © 2015 Wiley Periodicals, Inc.

DOI: 10.1002/qua.24902

Introduction

A detailed molecular level understanding of the ion-water interaction, especially of anion-water, is important due to its occurrence as an important reactive intermediate in many chemical processes ranging from atmospheric, biological to chemical reactions.^[1,2] Hydration of anion modifies the hydrogen-bonded network between water molecules and the extent of modification depends on the nature of anions.^[3-6] Various experimental and theoretical studies have been performed to acquire the molecular level understanding about the hydration of ions.^[7-12] Infrared (IR) photo-dissociation spectroscopy of size-selected clusters along with mass spectroscopic techniques have been important experimental tools to probe the structure of anions at various level of hydration.^[13-20] Experimental and theoretical tools have been complementarily applied for the microhydration study of various triatomic and more complex organic anions which feature a triatomic binding site.^[3-5,18-29]

Carbonyl sulfide (OCS) is the most abundant and stable sulfur-containing triatomic gas in the atmosphere which plays an important role in the aerosol formation.^[30,31] However, its anionic form (OCS^-) is a metastable species. Indeed, in one of the mass spectroscopic studies, OCS^- was not observed on the photodissociation of OCS which was attributed to its negative adiabatic electron affinity (AEA).^[32-37] The energy difference between the optimized neutral and optimized anionic state of a molecule is known as the AEA. A negative AEA implies that the relaxed neutral species lies lower in energy than the corresponding anion. In the same experimental study, the hydrated cluster anions of OCS^- , including in particular monohydrated OCS^- as well as larger cluster ions were produced readily and in abundance.^[35,36] The existence of mono-

hydrated anion indicates that OCS^- is stabilized by hydration. One interesting feature of OCS^- is the existence of both oxygen and sulfur atoms which can form $\text{O}-\text{H}\cdots\text{O}$ and $\text{O}-\text{H}\cdots\text{S}$ hydrogen bonds, respectively, with water and thereby, stabilize the OCS^- . In this context, an obvious question that evokes is that how water molecules bind with the OCS^- on sequential hydration and how microhydration affects the stability of the OCS^- . However, there is a dearth of literature on systematic experimental/theoretical studies, wherein the structure, stabilization energy, and IR spectrum of microhydrated OCS^- have been reported.

In this article, we have performed a theoretical study on the microhydration of OCS^- to understand the effect of hydration on the structure, energetics, and vibrational frequency of metastable OCS^- . Our results show that for $n = 1, 2$ clusters, water binds with OCS^- by $\text{O}-\text{H}\cdots\text{S}$ and $\text{O}-\text{H}\cdots\text{O}$ hydrogen bonds either single hydrogen-bonded (SHB) or double hydrogen-bonded (DHB) fashion, and the stability of DHB water is found to be higher compared with its singly bonded analogue. It is found that a maximum of two water molecules can directly bind with OCS^- in DHB arrangement. Most of the minimum energy configurations in $\text{OCS}^-(\text{H}_2\text{O})_n$ clusters show surface structure in which OCS^- resides at the surface of water network. Stabilization energies of $\text{OCS}^-(\text{H}_2\text{O})_n$ clusters depict that each water molecule stabilizes the OCS^- by 12.7 kcal/mol. This clearly substantiates that sequential addition of water

S. Mondal, A. Uday Teja and P. Chandra Singh

Department of Spectroscopy, Indian Association for the Cultivation of Science, Kolkata, 700032, West Bengal, India

E-mail: sppcs@iacs.res.in

Contract grant sponsor: Indian Association for the Cultivation of Science (IACS).

© 2015 Wiley Periodicals, Inc.

lowers the energy of the anion relative to the neutral state and hence, provides the stability to the hydrated clusters. IR spectra of the microhydrated OCS^- show that the number of overlapping bands in the OH stretching region of water molecule increases with increase in the number of water molecules revealing that the stretching modes of water are very strongly coupled with each other for higher order of clusters. The CO and CS stretching frequencies of OCS^- moiety in the hydrated clusters have been explored to understand the effect of microhydration on the OCS^- . It is found that the CO stretching frequency of OCS^- gets red shifted, whereas CS stretching frequency gets blue shifted on the hydration.

Methodology

All the structures of microhydrated OCS^- have been optimized at the MP2 level of theory with 6-311++G(d, p) basis set. To confirm the nature of stationary points, subsequent harmonic frequency calculations have been performed for the corresponding optimized structures. To get the accurate energetics, we have performed single point calculation at the CCSD (T)/6-311++G(d, p) level of theory for all the structures up to four water clusters of OCS^- , optimized at the MP2/6-311++G(d, p) level. The energetic value calculated at the CCSD (T) level of theory provides similar value as to the MP2 level of calculation, which shows that the MP2/6-311++G(d, p) level of calculation is indeed a reliable method for the structure and energy calculation of $\text{OCS}^-(\text{H}_2\text{O})_n$ clusters. Unrestricted optimization method has been used for the anions, whereas neutral systems have been optimized with restricted approach. The values of the spin contamination $\langle S^2 \rangle$ are found to be ~ 0.768 which is quite close to the acceptable value of 0.75 for the pure doublet system. All the above calculations have been performed with frozen core approximation and optimization has been done with standard convergence criteria. Energies have been corrected for the basis set superposition error (BSSE) by the counterpoise method. Charge on the different atoms of monomer and hydrated OCS^- has been calculated by the CHELPG scheme.

Several initial structures have been designed based on the chemical intuitions and optimization of these structures has been performed to find the minimum energy structure. The most important concern in this process is to guess a good initial structure which can easily converge to a local or global minimum. Different initial guess structures were designed based on the possible three-dimensional arrangements of water molecules around the OCS^- . Initial guess structures have been first optimized with the HF/6-31+G(d) level of theory and then, the optimized structure of this calculation has been used as an initial structure for the MP2/6-311++G(d, p) level of optimization. The initial guess structures for the monohydrate cluster of OCS^- were prepared by keeping the water first on the oxygen, followed by the sulfur-binding site in single as well as in DHB mode. The guess structures were also prepared by changing the plane of hydrogen bonding, that is, in-plane or out-of-plane of OCS^- . Four minimum energy structures were found for the monohydrated cluster of

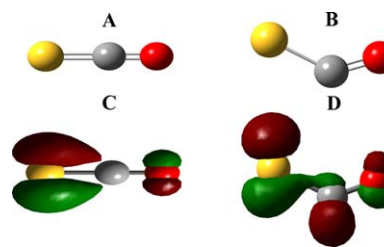


Figure 1. The stable structures of the OCS (A) and OCS^- (B) at the MP2/6-311++G(d, p) level of theory. HOMO of OCS and OCS^- have been shown in (C) and (D) respectively, at the MP2/6-311++G(d, p) level of theory. Oxygen, hydrogen, and sulfur atoms are depicted in red, black, and yellow, respectively.

OCS^- . The number of minimum energy conformers is expected to be high for a larger size of hydrated clusters. The initial structures for large size clusters were prepared with the bottom-up approach based on the structures of smaller clusters. For example, to find maximum number of possible minimum energy structures of the dihydrated OCS^- , we have first taken the most stable structure of monohydrated OCS^- followed by the addition of subsequent water to the entire possible binding sites and the same procedure has been followed with other stable structures of the monohydrated OCS^- . However, by this approach, it cannot be claimed that all the possible stable conformers of any particular size of cluster have been achieved and there is always possibility that some stable structures may be missed during this calculation.

The number of minimum energy structures within close energy range increases with increase in the number of water molecules, hence, it is meaningful to calculate the weighted average molecular properties. Molecular properties such as vibrational frequency, interaction energy, and solvent stabilization energy have been calculated in terms of weighted average values. The weight factor is calculated based on the computed free energy change (ΔG) which provides the relative population for each of the conformers of different sizes of hydrated clusters. All the above calculations have been performed by the Gaussian 09 suites of program.^[38]

Results and Discussion

Figure 1 shows the most stable structures of OCS and OCS^- along with their corresponding highest occupied molecular orbital (HOMO) calculated at the MP2/6-311++G(d, p) level of theory. The important geometrical parameters, electronic energy, and charges on different atoms of OCS and OCS^- calculated at the MP2/6-311++G(d, p) level of theory have been shown in Table 1. OCS is a linear molecule with double bond character of CO and CS bonds.^[39] In contrast, OCS^- is bent with more elongated CO and CS bonds. AEA for the OCS is calculated at the MP2 and CCSD(T) level of theories and found to be -0.59 and -0.34 eV, respectively. Calculated AEA values of OCS at the both level of theories are higher as compared with the earlier reported AEA value for OCS (-0.059 eV) by Sanov and coworkers.^[35] Hence, we have also calculated the AEA at the G3 level and the value was found to be -0.059 eV

Table 1. The Electronic energy (atomic unit), CO, CS distance (Å), OCS angle (degree), and charges (atomic unit) on the oxygen, carbon, and sulfur atom of OCS as well as OCS[−] calculated at the MP2/6-311++G(d, p) level of calculation.

	Electronic energy	CO	CS	OCS	q^O	q^C	q^S
OCS	−510.7721826 (−510.7981783)	1.17	1.56	180.0	−0.241	0.343	−0.102
OCS [−]	−510.7506822 (−510.7856101)	1.22	1.69	135.3	−0.386	0.018	−0.631

q^O , q^C , and q^S represent the charges on the oxygen, carbon and sulfur atom, respectively calculated by the CHELPG scheme. The calculated value of electronic energies at the G3 level of theory for OCS and OCS[−] are −511.346644 and −511.344473, respectively.

which is in accordance to the earlier reported value of AEA.^[35] Charge analysis points out that the addition of electron to OCS increases the negative charge more on the sulfur which is also evident from the HOMO of OCS and OCS[−].

Figure 2 shows the most stable structure along with all other minimum energy conformers of OCS[−]-(H₂O)_n clusters calculated at the MP2/6-311++G(d, p) level of theory. The absolute and their relative energy (energy difference between that specific structure with the most stable structure for a particular size of cluster) of all the conformers of OCS[−]-(H₂O)_n calculated at the MP2/6-311++G(d, p) level of theory have been provided in the Supporting Information (Table S1). Four stable minimum energy structures have been found for the monohydrated cluster of OCS[−] as shown in Figure 2 (A1 to A4). The most stable structure (A1) of monohydrated OCS[−] has an asymmetric DHB arrangement of water in which both OH group of water molecule is donor and hydrogen bonded to oxygen and sulfur of OCS[−]. The O—H...O and O—H...S distances for A1 are 2.12 and 2.49 Å, respectively. The CO and CS bond distances are 1.22 and 1.69 Å, respectively. Structure A2 consists of SHB water molecule with O—H...S hydrogen bond arrangement and the O—H...S, CO, and CS distances are 2.34, 1.21, and 1.70 Å, respectively. Structure A3 is in-plane O—H...O hydrogen-bonded complex in which O—H...O, CO, and CS distances are 1.86, 1.23, and 1.68 Å, respectively. Structure A4 is out-of-plane O—H...O hydrogen-bonded complex where O—H...O distance is 1.91 Å and CO, CS distances are 1.22, 1.68 Å, respectively. The O—H...O distances for A3 and A4 are lower in comparison to A1, but their relative energies are less by ~2–4 kcal/mol in comparison to A1. Similarly, O—H...S distance for A2 is lower compared with A1, also the relative energy is slightly less (1 kcal/mol) in comparison to A1. The higher stability of DHB structure (A1) of monohydrated OCS[−] is due to fact that the bent OCS[−] has proper O...S distance (2.70 Å) to accommodate the water in DHB arrangement, similar to the case of water trimer.^[40] We have also calculated the electronic energies for A1 and A2 at the G3 level of theory and the energy difference between these two structures is found to be 1.9 kcal/mol, which is quite close to the calculated value at the MP2 (1.42 kcal/mol) and CCSD(T) (1.75 kcal/mol) level of theories. One of the earlier calculations for the monohydrated OCS[−] performed at the CCSD/6-311++G(d, p) level of theory found identical stable structures

as of our present calculations which illustrates that the MP2/6-311++G(d, p) level of calculation is appropriate for further structure and energy calculations.³⁵

Seven minimum energy structures have been found for the dihydrated OCS[−] cluster as shown in Figure 2 (B1 to B7). Two different trends of structures have been observed for the dihydrated OCS[−]. In the first trend, first water is asymmetrically DHB to OCS[−] (similar to A1) and subsequent water is found to interact in three different ways. In the first mode, second water is bonded to first water by interwater hydrogen bonding (IHB) and also interacts with the sulfur terminal of OCS[−] (B1). In other modes, either second water is only IHB to first water (B2) or interacts to OCS[−] in DHB fashion (B5). In the second trend, two water molecules are connected by IHB and also interact with OCS[−] in SHB fashion (B3, B4, B6, and B7). B1 and B2 are almost isoenergetic and most stable structures. Other structures are energetically close with a relative energy difference of ~3 kcal/mol. In general, the O—H...O and O—H...S distances for dihydrated complexes are less as compared with monohydrated complexes and maximum and minimum values of O—H...O, O—H...S distances are 2.75, 1.78, 2.63, and 2.23 Å, respectively.

For the preparation of initial structures of the trihydrated OCS[−], water has been added to the entire possible binding configurations of the most stable structure of dihydrated OCS[−] and same procedure has been followed with other stable structures of dihydrated OCS[−]. Total 16 stable minimum energy structures have been found for the trihydrated OCS[−], out of which, 10 lowest minimum energy structures have been shown in Figure 2 (C1–C10). Structures of all the stable conformers have been shown in the Supporting Information (Fig. S1[C1–C16]). In the first trend, one or two water molecules are DHB with OCS[−] and rest of the water molecules are IHB with each other. These IHB water molecules are either only interacting with DHB water molecules or with oxygen/ sulfur termini of OCS[−] (C1, C5, C6, C8, C9, C11, C12, C14, and C16). For example, two water molecules of C1 structure have DHB with OCS[−] and third water is IHB with these two water molecules, whereas for C5, one water molecule has DHB with OCS[−] and remaining two water molecules have IHB as well as hydrogen bonded with first water molecule. In other structures, all water molecules are IHB with each other and also hydrogen bonded with either oxygen or sulfur terminal of OCS[−] in SHB fashion (C2, C3, C4). C1 and C2 are the most stable structures with similar energy. The energies of other conformers are within ~6 kcal/mol relative to the most stable conformer.

Optimization of OCS[−]-(H₂O)₄ yields total 32 stable structures, out of which, 10 most stable structures have been depicted in Figure 2 (D1–D10). Full list of the stable structures have been shown in the Supporting Information (Fig. S1 [D1–D32]). Most stable structure of OCS[−]-(H₂O)₄ (D1) has one DHB water with OCS[−] and rest four water molecules are IHB with each other. The least stable structure (D32) comprises two different sets of water dimers attached with oxygen and sulfur termini of OCS[−], respectively. Among other most stable structures, most prominent are those in which water is hydrogen bonded with each other in cyclic fashion and two/three

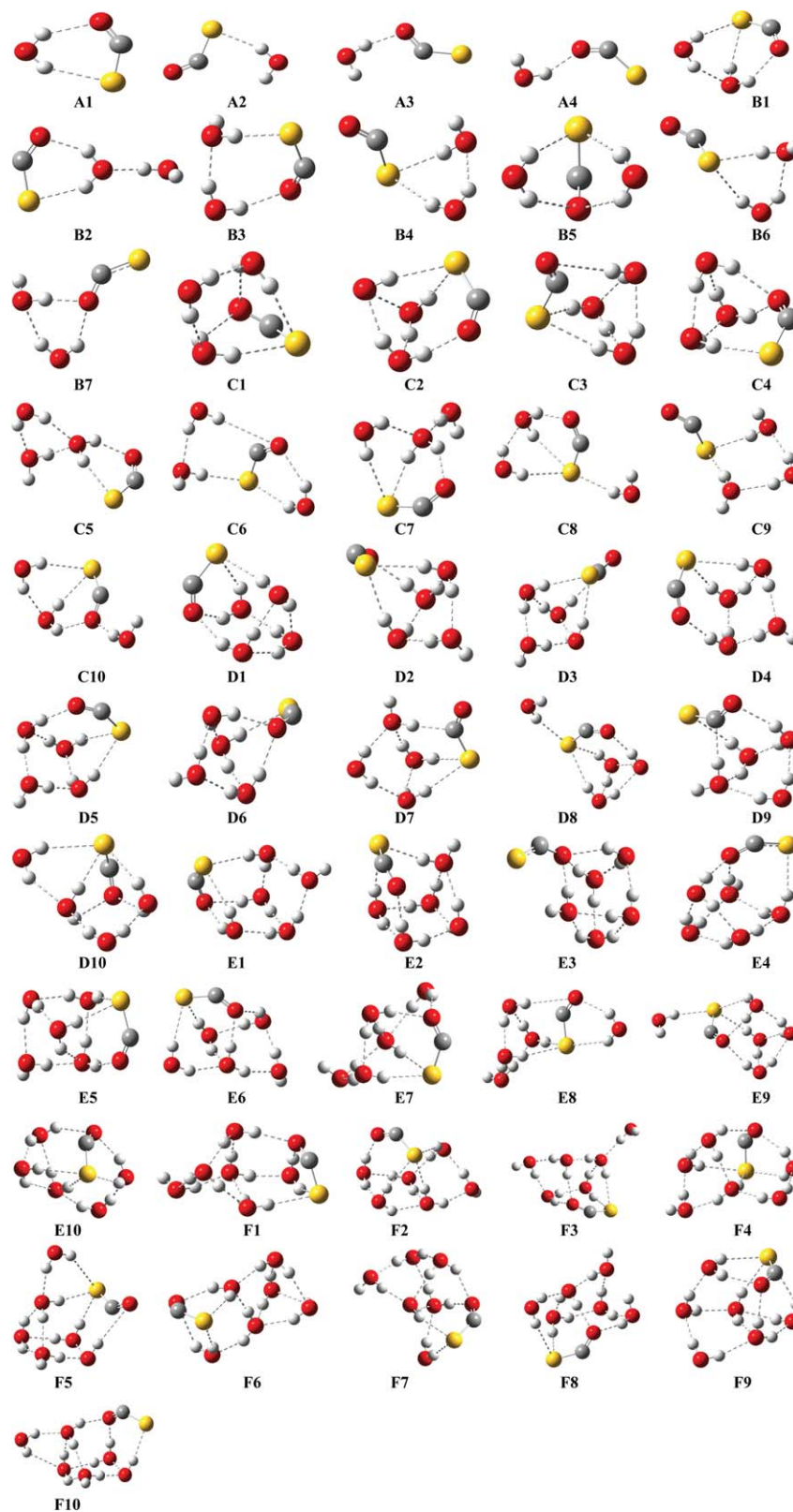


Figure 2. Optimized minimum energy structures of $\text{OCS}^- - \text{H}_2\text{O}$ (A1–A4), $\text{OCS}^- - 2\text{H}_2\text{O}$ (B1–B7), $\text{OCS}^- - 3\text{H}_2\text{O}$ (C1–C10), $\text{OCS}^- - 4\text{H}_2\text{O}$ (D1–D10), $\text{OCS}^- - 5\text{H}_2\text{O}$ (E1–E10), and $\text{OCS}^- - 6\text{H}_2\text{O}$ (F1–F10), respectively at the MP2/6-311++G(d, p) level of theory. Oxygen, hydrogen, carbon, and sulfur atoms are depicted in red, white, black, and yellow, respectively.

water molecules are interacting with the OCS^- in SHB/DHB fashion (D2–D9). The energy difference between two most stable structures (D1, D2) is 0.5 kcal/mol. Other structures are close in energy to the most stable structure with a maximum difference of ~ 7 kcal/mol.

The optimization of $\text{OCS}^-(\text{H}_2\text{O})_5$ provides 27 stable structures, out of which, 10 most stable structures have been shown in Figure 2 (E1–E10) and full list of structures have been depicted in the Supporting Information (Fig. S1[E1–E27]). E1 and E2 are almost isoenergetic and most stable ones. E1 has one water molecule interacting with OCS^- in DHB manner and rest four water molecules are in cyclic hydrogen-bonded network. E2 has one cyclic five water network forming IHB with each other and three water molecules in this cyclic network are hydrogen bonded with OCS^- moiety. The least stable structure has a chain like network of water containing two DHB and SHB as well as water molecules are IHB with each other. The energy difference between the most stable and least stable energy conformer is ~ 6 kcal/mol. One interesting observation is that maximum stable structures keep the solute anion at the interface and growth of the solvent involves hydrogen bonding with oxygen and sulfur of OCS^- .

Full optimization of $\text{OCS}^-(\text{H}_2\text{O})_6$ yields total 25 stable structures, of which, 10 most stable structures have been depicted in Figure 2 (F1–F10) and complete list of the stable structures has been reported in the Supporting Information (Fig. S1[F1–F25]). The most stable structure F1 has five water hydrogen bonded with each other in IHB fashion and the remaining water is DHB to the OCS^- . Different arrangements of IHB between water molecules have been found for different structures, however, solute is always at the surface and the formation of hydrogen-bonded water network takes place at the top/bottom/side excepting for F17, F19, and F21. OCS^- is trapped inside the hydrogen-bonded water network for F17, F19, and F21. Nevertheless, their relative stability is less (~ 5 – 6 kcal/mol) as compared with the surface structure. The energy difference between the most stable and least stable energy conformer is ~ 8 kcal/mol. The stability of higher $\text{OCS}^-(\text{H}_2\text{O})_n$ ($n > 3$) complexes depend on the subtle balance between the IHB of water molecules and their interaction with the OCS^- .

The CO and CS distances are in the range of 1.21–1.23 and 1.67–1.70 Å, respectively, for all the stable structures of $\text{OCS}^-(\text{H}_2\text{O})_n$. Hydrogen bonding distances for $\text{O} \cdots \text{H} \cdots \text{O}$ and $\text{O} \cdots \text{H} \cdots \text{S}$ are in the range of 1.78–2.10 and 2.25–2.73 Å, respectively, for all the hydrated clusters. The average IHB between the water molecules for all the microsolvated clusters is in between 1.8 and 2.1 Å. In general, the calculated SHB distances are shorter than that of DHB distances for all the stable structures. Cyclic IHB network between the water molecules is more stable over other structures for a particular size of hydrated clusters. For small water clusters, water binds with OCS^- by $\text{O} \cdots \text{H} \cdots \text{O}$ and $\text{O} \cdots \text{H} \cdots \text{S}$ hydrogen bonds. Maximum five water molecules can stay in the cyclic water network of these hydrated clusters forming IHB with each other and out of this, maximum of two water molecules can bind directly to OCS^- in double hydrogen bonding arrangement. Most of the minimum energy configurations in $\text{OCS}^-(\text{H}_2\text{O})_n$ clusters

show surface structure in which the OCS^- resides at the surface of the water network. In some structures of large water clusters, OCS^- resides in the interior of the water network, rendering lesser stability.

Solvent stabilization and interaction energy

Solvent stabilization (E^{solv}) and interaction (E^{int}) energies are two important parameters which have been frequently used to understand the stabilization of solute by solvents in discrete solvent model.^[25,41,42] E^{solv} measures the total interaction energy of the solute with n water molecules in the microhydrated cluster of size n , whereas interaction energy denotes the net interaction of the solute and solvent water molecules eliminating the contribution of IHB. The solvent stabilization energy is the energy which is induced by the water molecule for the $\text{OCS}^-(\text{H}_2\text{O})_n$ clusters and has been calculated by the following equation

$$E^{\text{solv}} = E(\text{OCS}^-[\text{sbond}]n\text{H}_2\text{O}) - [E(\text{OCS}^-) + nE(\text{H}_2\text{O})],$$

where $E(\text{OCS}^-n\text{H}_2\text{O})$, $E(\text{OCS}^-)$, $E(\text{H}_2\text{O})$ represent the total energy of the cluster $\text{OCS}^-(\text{H}_2\text{O})_n$, energy of the OCS^- and water monomer, respectively. Interaction energy corresponds to the net interaction of solute OCS^- with solvent water molecule in the absence of IHB between the water molecules and is calculated by the following relation

$$E^{\text{int}} = E(\text{OCS}^-[\text{sbond}]n\text{H}_2\text{O}) - [E(\text{OCS}^-)_s + E(\text{H}_2\text{O})_n],$$

where $E(\text{OCS}^-n\text{H}_2\text{O})$ represent the total energy of the cluster $\text{OCS}^-n\text{H}_2\text{O}$. $E(\text{H}_2\text{O})_n$ has been obtained from a single point calculation for the $(\text{H}_2\text{O})_n$ after removing the OCS^- from the optimized geometry of particular cluster. Similarly, $E(\text{OCS}^-)_s$ is obtained from a single point energy calculation of the OCS^- after removing the $(\text{H}_2\text{O})_n$ from the optimized geometry of that particular cluster.

Table 2 shows the solvent stabilization energies for all the structures of $\text{OCS}^-(\text{H}_2\text{O})_n$ calculated at the MP2 and CCSD(T) level of methods with 6-311++G(d, p) basis set. It has been observed that the solvent stabilization energy increases with the addition of water molecules. The values of solvent stabilization energy calculated at the CCSD(T) level of theory (Table 2) are very close to MP2 results. It is not possible to discuss distinctly about the stability provided to each conformer by the addition of successive water molecules due to the existence of several near energy conformers. Hence, we have calculated the weighted average solvent stabilization energy for $\text{OCS}^-(\text{H}_2\text{O})_n$ at the MP2/6-311++G(d, p) level of theory and the values are shown in Table 3. The value of weighted average solvent stabilization energy indicates that the addition of one water molecule stabilizes the OCS^- by ~ 13 kcal/mol. Figure 3 shows the change in the weighted average solvent stabilization energy of $\text{OCS}^-(\text{H}_2\text{O})_n$ with respect to the number of water molecules in the particular cluster. It is clearly observed that the weighted average solvent stabilization energy varies linearly with the number of water

Table 2. Calculated energy parameters of $\text{OCS}^--(\text{H}_2\text{O})_n$ ($n = 1-6$) clusters.

	Interaction energy (kcal/mol)	Solvent stabilization energy (kcal/mol)	Interaction energy (kcal/mol)	Solvent stabilization energy (kcal/mol)
System	MP2/6-311++G (d, p)		CCSD(T)/6-311++G(d, p)	
1W				
A1	15.6 (12.9)	15.2 (12.5)	15.7 (12.7)	15.5 (12.5)
A2	14.2 (11.8)	13.8 (11.3)	13.8 (11.2)	13.7 (11.1)
A3	13.2 (11.6)	12.8 (11.1)	13.3 (11.5)	13.0 (11.1)
A4	11.7 (10.0)	11.4 (9.7)	11.9 (10.2)	11.7 (9.9)
2W				
B1	26.9 (22.3)	28.3 (22.5)	26.8 (21.9)	28.9 (22.7)
B2	22.7 (19.2)	27.4 (22.0)	22.8 (19.0)	27.8 (22.2)
B3	23.9 (20.1)	27.3 (22.1)	23.8 (19.7)	27.7 (22.1)
B4	25.8 (21.3)	27.1 (21.4)	25.1 (20.4)	27.2 (21.2)
B5	28.6 (23.6)	26.5 (21.1)	28.6 (23.3)	27.1 (21.4)
B6	24.1 (19.7)	25.5 (19.8)	23.5 (18.8)	25.6 (19.7)
B7	23.8 (20.9)	24.9 (20.8)	23.9 (20.8)	25.5 (21.2)
3W				
C1	33.3 (27.8)	42.0 (33.2)	33.1 (27.3)	42.8 (33.6)
C2	37.2 (31.6)	41.7 (33.0)	37.1 (31.1)	42.5 (33.4)
C3	34.1 (28.7)	41.5 (32.9)	33.2 (27.5)	41.8 (32.8)
C4	32.4 (27.5)	41.0 (32.8)	32.5 (27.3)	42.0 (33.4)
C5	30.6 (26.4)	39.9 (31.6)	30.6 (26.0)	40.5 (31.9)
C6	37.7 (28.3)	39.6 (31.6)	37.2 (30.5)	39.9 (30.7)
C7	35.0 (31.4)	39.6 (31.9)	34.8 (29.1)	40.3 (31.8)
C8	38.7 (25.9)	39.4 (31.4)	38.4 (31.7)	40.0 (31.2)
C9	33.6 (29.6)	39.3 (31.2)	32.7 (27.2)	39.5 (31.5)
C10	38.5 (32.4)	39.0 (31.9)	38.4 (32.1)	39.7 (32.1)
4W				
D1	41.6 (35.1)	55.6 (43.7)	41.7 (34.8)	56.8 (44.4)
D2	34.4 (28.5)	55.0 (42.7)	34.2 (28.0)	55.8 (43.0)
D3	35.0 (29.4)	54.2 (42.2)	34.2 (28.2)	54.5 (42.0)
D4	33.2 (27.6)	54.2 (42.1)	33.1 (27.1)	55.0 (42.4)
D5	32.9 (27.4)	54.0 (42.0)	32.8 (26.9)	54.9 (42.2)
D6	33.6 (28.4)	53.8 (42.2)	33.8 (28.3)	54.9 (42.7)
D7	41.2 (35.2)	52.9 (41.7)	40.1 (33.8)	53.2 (41.5)
D8	44.4 (33.5)	52.6 (41.6)	43.9 (36.6)	53.5 (41.5)
D9	39.1 (37.5)	52.4 (42.3)	38.3 (32.5)	52.8 (41.9)
D10	47.0 (33.6)	52.3 (41.6)	46.7 (39.4)	53.4 (42.7)
5W				
E1	42.1 (35.5)	68.5 (53.0)		
E2	41.1 (34.7)	68.5 (53.1)		
E3	44.7 (39.2)	67.6 (53.7)		
E4	44.3 (37.9)	67.2 (52.8)		
E5	39.7 (33.2)	67.2 (51.4)		
E6	42.0 (35.3)	66.0 (51.3)		
E7	44.3 (35.4)	65.9 (51.3)		
E8	46.6 (37.0)	65.8 (51.1)		
E9	52.6 (39.4)	65.8 (52.1)		
E10	51.0 (44.4)	65.7 (52.2)		
6W				
F1	45.2 (38.4)	79.8 (61.7)		
F2	44.9 (37.8)	79.4 (61.2)		
F3	44.5 (41.0)	79.2 (61.2)		
F4	50.2 (42.4)	78.8 (61.1)		
F5	46.4 (39.3)	78.8 (60.9)		
F6	49.5 (43.2)	78.7 (61.5)		
F7	46.1 (39.0)	78.3 (60.5)		
F8	45.6 (38.4)	78.2 (60.6)		
F9	55.5 (47.7)	78.1 (60.9)		
F10	42.4 (36.2)	77.6 (60.4)		
Interaction energy (kcal/mol) and solvent stabilization energy (kcal/mol) have been calculated at the MP2 and CCSD(T) methods with 6-311++G (d, p) basis set. BSSE corrected energies at the respective level of theories have been depicted in brackets.				

Table 3. Weighted average solvent stabilization and interaction energy (kcal/mol) for the $\text{OCS}^-(\text{H}_2\text{O})_n$ ($n = 1-6$) clusters calculated at the MP2/6-311++ G(d, p) level of theory.

	Weighted average energies (kcal/mol)	
	Solvent stabilization energy	Interaction energy
$\text{OCS}^--\text{H}_2\text{O}$	14.6 (12.0)	15.0 (12.3)
$\text{OCS}^--2\text{H}_2\text{O}$	27.4 (21.9)	24.6 (20.6)
$\text{OCS}^--3\text{H}_2\text{O}$	39.6 (31.6)	36.2 (30.5)
$\text{OCS}^--4\text{H}_2\text{O}$	51.1 (40.8)	44.9 (38.1)
$\text{OCS}^--5\text{H}_2\text{O}$	65.0 (51.0)	47.0 (40.1)
$\text{OCS}^--6\text{H}_2\text{O}$	78.2 (60.7)	47.6 (42.0)

The values shown in the bracket correspond to the BSSE corrected energies.

molecules and the plot can nicely be fitted with the equation $y = 12.7n + 1.78$, where y is weighted average solvent stabilization energy (kcal/mol) and n is the number of water molecules. The slope of line indicates that the average solvent stabilization energy increases by 12.7 kcal/mol with the addition of successive water molecules. This implies that each additional hydrogen bond provides energy of 6.35 kcal/mol, assuming that each water molecule increases the number of hydrogen bonds by two. The electronic energy of OCS^- is found to be 13 kcal/mol higher in comparison to the neutral OCS molecule at the MP2 level of theory. Addition of single water molecule provides a stability of 12.7 kcal/mol to the OCS^- and the energy becomes almost equal to the neutral OCS molecule. Successive water addition makes the $\text{OCS}^-(\text{H}_2\text{O})_n$ clusters more stable as compared with OCS^- [35,36].

Table 2 shows the values of interaction energies for each structure of $\text{OCS}^-(\text{H}_2\text{O})_n$ clusters calculated at the MP2/6-311++G(d, p) level of theory and the values of weighted average interaction energies are depicted in Table 3. The interaction energies values calculated at CCSD(T) level of theory for $\text{OCS}^-(\text{H}_2\text{O})_n$ clusters up to four water molecules (Table 2) are found to be similar to the MP2 level of theory. The variation of the weighted average interaction energy with the number of water molecules are depicted in Figure 3. Weighted average interaction and solvent stabilization energies are found to be approximately same for monohydrated complexes of OCS^- , whereas weighted average solvent stabilization energy is slightly higher as compared with weighted average interaction energy for $n = 2, 3$ clusters. The trend of data for weighted average solvent stabilization and interaction energy indicates that the IHB has small contribution for $n = 2, 3$ cluster. The important feature of the weighted average interaction energy is that it increases up to four water molecules and gets saturated beyond that. This suggests that interaction of OCS^- with water molecules is prominent up to four water molecules implying that the first half solvation shell of OCS^- contains up to four water molecules. Half solvation shell is assumed because OCS^- is at the interface and growth of water network takes place in one direction. Weighted average solvent stabilization energy increases linearly with the number of water molecules due to the fact that solvent stabilization energy

includes the ion-solvent interaction along with IHB hence, does not get saturated and remains favorable to attach additional water molecules in the existing hydrogen-bonded water network. BSSE-corrected values of energies (Tables 3 and 4) clearly show that BSSE correction does not change the trend *albeit* only decrease the values by $\sim 5-10\%$ as depicted in Figure 3.

Vibrational frequency

$\text{OCS}^-(\text{H}_2\text{O})_n$ clusters are stabilized by the $\text{O}-\text{H}\cdots\text{O}$ and $\text{O}-\text{H}\cdots\text{S}$ hydrogen bonding along with IHB between the water molecules. It is well known that vibrational spectroscopy of donor groups are very sensitive to hydrogen-bonded structures and show characteristic frequency shifts on hydrogen bonding.^[43] It is expected that different structures for the same or different hydration levels shall change the bending and stretching frequencies of water differently as compared with free water. The vibrational frequencies of $\text{OCS}^-(\text{H}_2\text{O})_n$ clusters along with monomers have been calculated at the MP2/6-311++G(d, p) level of theory to understand the effect of hydration on the stretching and bending of water molecule. To get the microscopic picture of vibrational frequency, weighted average IR spectra have been calculated for the $\text{OCS}^-(\text{H}_2\text{O})_n$ clusters as the number of close energy conformers are considerably high.

The calculated harmonic OH stretching frequencies ($\nu_{\text{symmetric}} = 3885 \text{ cm}^{-1}$, $\nu_{\text{asymmetric}} = 4003 \text{ cm}^{-1}$) are higher as compared with their experimental values ($\nu_{\text{symmetric}} = 3657 \text{ cm}^{-1}$, $\nu_{\text{asymmetric}} = 3756 \text{ cm}^{-1}$) hence, a scaling factor of 0.94 has been used to account for the

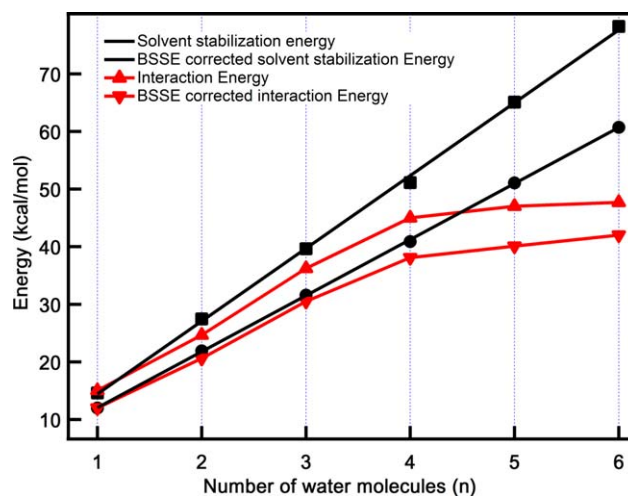


Figure 3. Plot of the weighted average solvent stabilization (black square) and interaction energy (red triangle) with respect to the number of water molecules (n) in the $\text{OCS}^-(\text{H}_2\text{O})_n$ clusters calculated at the MP2/6-311++G(d, p) level of theory. BSSE-corrected solvent stabilization and interaction energy are depicted in black circle and red inverted triangle, respectively. The black line represents the linear fit with equation $y = 12.7n + 1.78$ where y is weighted average solvent stabilization energy (kcal/mol) and n is the number of water molecule. The value of correlation coefficient was found to be 0.9996 which reflects high reliability of the fitting. The red line is only an eye guide line for the interaction energy (kcal/mol) change with respect to the number of water molecule.

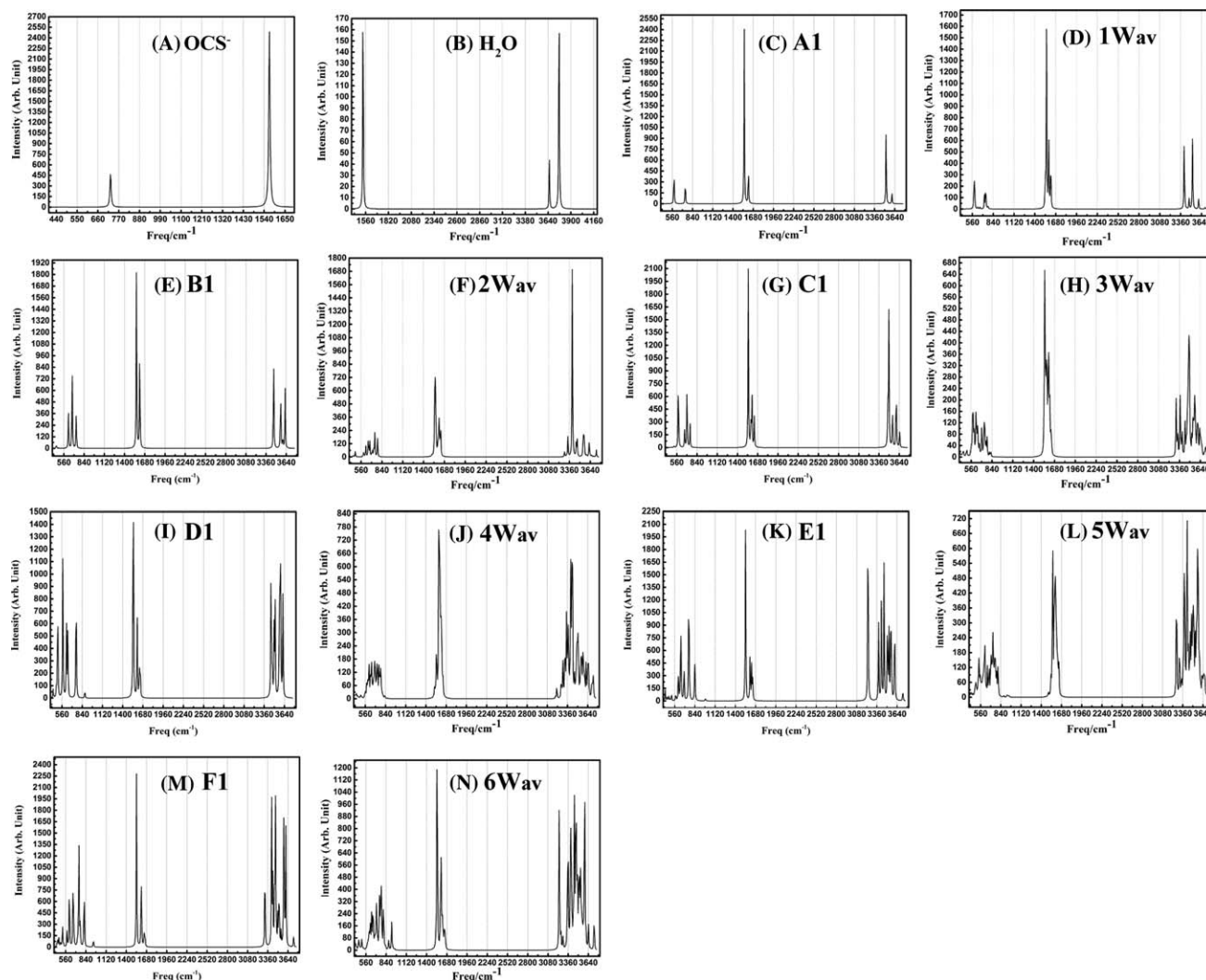


Figure 4. Scaled IR spectra for the H_2O (A) and OCS^- (B) monomer at the MP2/6-311++G(d, p) level of calculation. The scaled IR spectra for the most stable structures of $\text{OCS}^- \text{--} \text{H}_2\text{O}$ (C), $\text{OCS}^- \text{--} 2\text{H}_2\text{O}$ (E), $\text{OCS}^- \text{--} 3\text{H}_2\text{O}$ (G), $\text{OCS}^- \text{--} 4\text{H}_2\text{O}$ (I), $\text{OCS}^- \text{--} 5\text{H}_2\text{O}$ (K), and $\text{OCS}^- \text{--} 6\text{H}_2\text{O}$ (M), respectively calculated at the MP2/6-311++G (d, p) level of theory. The scaled weighted average IR spectra for the $\text{OCS}^- \text{--} \text{H}_2\text{O}$ (D), $\text{OCS}^- \text{--} 2\text{H}_2\text{O}$ (F), $\text{OCS}^- \text{--} 3\text{H}_2\text{O}$ (H), $\text{OCS}^- \text{--} 4\text{H}_2\text{O}$ (J), $\text{OCS}^- \text{--} 5\text{H}_2\text{O}$ (L), and $\text{OCS}^- \text{--} 6\text{H}_2\text{O}$ (N), respectively, at the same level of theory. The scaling factor of 0.94 has been used to account the anharmonicity for the OH stretching vibration of water molecule.

anharmonic nature of OH stretching vibrations. The scaling factor is calculated on the basis of average difference between the calculated symmetric and asymmetric stretching vibration frequencies to the experimental one. Same scaling factor has been used for the calculation of other vibrational modes for all the structures of $\text{OCS}^- \text{--} (\text{H}_2\text{O})_n$. Table 4 depicts the scaled OH stretching frequencies of water monomer as well as water in the most stable structures of $\text{OCS}^- \text{--} (\text{H}_2\text{O})_n$ clusters obtained at the MP2/6-311++G(d,p) level of theory. The scaled IR spectrum of the most stable structures along with the weighted average IR spectrum of $\text{OCS}^- \text{--} (\text{H}_2\text{O})_n$ clusters (from 400 to 4000 cm^{-1} covering the OH stretching, bending, CO and CS stretching frequencies) are shown in Figure 4. The scaled CO and CS stretching frequencies of OCS^- are 1567 and 727 cm^{-1} , respectively, and spectral feature at $\sim 600 \text{ cm}^{-1}$ belongs to the OCS bending as depicted in Figure 4a. The scaled symmetric, asymmetric and bending frequency values for water monomer are 3652, 3763, and 1531 cm^{-1} , respec-

tively, as shown in Figure 4b. The symmetric, asymmetric stretching, and bending frequencies of water in the conformer A1 of the $\text{OCS}^- \text{--} \text{H}_2\text{O}$ cluster are at 3520, 3600, and 1613 cm^{-1} , respectively, (Table 4, Fig. 4c). The stretching frequencies of water in A1 are red shifted ($\Delta\nu_{\text{symmetric}} = -132 \text{ cm}^{-1}$, $\Delta\nu_{\text{asymmetric}} = -163 \text{ cm}^{-1}$), whereas bending is blue shifted ($\Delta\nu_{\text{bending}} = +82 \text{ cm}^{-1}$) as compared with the water monomer. It has been shown for many systems that hydrogen bonding causes red shift in the stretching frequency and blue shift to the bending of water.^[44] The observed shift of water stretching and bending frequency for conformer A2 are $\Delta\nu_{\text{symmetric}} = -245 \text{ cm}^{-1}$, $\Delta\nu_{\text{asymmetric}} = -75 \text{ cm}^{-1}$, $\Delta\nu_{\text{bending}} = +76 \text{ cm}^{-1}$, respectively. The shift of $\Delta\nu_{\text{symmetric}}$ is higher for A2 as compared with the A1, whereas the $\Delta\nu_{\text{asymmetric}}$ for A1 is higher compared with the free OH of A2. These vibrational features for A1 and A2 nicely manifest their respective structures. In A1, water is DHB with OCS^- due to which both OH stretching of water gets

Table 4. Scaled OH stretching frequencies (cm^{-1}) of water as well as scaled CO, CS stretching frequencies and bending frequencies (cm^{-1}) of OCS^- in the $\text{OCS}^-(\text{H}_2\text{O})_n$ ($n = 1-6$) clusters at the MP2/6-311++ G(d, p) level of theory.

System	O—H stretching frequency					
H_2O	3652, 3763					
$\text{OCS}^-(\text{H}_2\text{O})$ (A1)	3520, 3600					
$\text{OCS}^-(2\text{H}_2\text{O})$ (B1)	3465, 3591, 3562, 3624					
$\text{OCS}^-(3\text{H}_2\text{O})$ (C1)	3481, 3495, 3547, 3599, 3643, 3646					
$\text{OCS}^-(4\text{H}_2\text{O})$ (D1)	3455, 3470, 3498, 3511, 3569, 3577, 3584, 3618					
$\text{OCS}^-(5\text{H}_2\text{O})$ (E1)	3237, 3383, 3424, 3460, 3507, 3527, 3553, 3564, 3606, 3719					
$\text{OCS}^-(6\text{H}_2\text{O})$ (F1)	3320, 3413, 3428, 3454, 3468, 3498, 3516, 3542, 3578, 3588, 3610, 3718					
	CO stretching	CS stretching	OCS bending	q^{O}	q^{S}	q^{C}
OCS^-	1567	727	476	−0.386	−0.631	0.018
$\text{OCS}^-(\text{H}_2\text{O})$ (A1)	1556	740	487	−0.449	−0.625	0.067
$\text{OCS}^-(2\text{H}_2\text{O})$ (B1)	1560	731	488	−0.432	−0.621	0.081
$\text{OCS}^-(3\text{H}_2\text{O})$ (C1)	1550	744	487	−0.435	−0.569	0.060
$\text{OCS}^-(4\text{H}_2\text{O})$ (D1)	1545	753	486	−0.410	−0.556	0.051
$\text{OCS}^-(5\text{H}_2\text{O})$ (E1)	1543	761	489	−0.418	−0.551	0.047
$\text{OCS}^-(6\text{H}_2\text{O})$ (F1)	1542	761	488	−0.412	−0.547	0.042

Charges (atomic unit) on the oxygen, carbon, and sulfur atom of OCS^- in the $\text{OCS}^-(\text{H}_2\text{O})_n$ ($n = 1-6$) clusters calculated at the MP2/6-311++G(d, p) level of theory. The scaling factor of 0.94 has been used to account the anharmonicity for the OH stretching vibration of water molecule. Same scaling factor has been used for the CO, CS stretching, and OCS bending frequency. q^{O} , q^{C} , and q^{S} represent the charges on the oxygen, carbon, and sulfur atoms, respectively calculated using the CHELPG scheme.

substantially red shifted as compared with free water, whereas A2 has one SHB of water for which $\Delta\nu_{\text{symmetric}}$ is comparatively high and $\Delta\nu_{\text{asymmetric}}$ is less because of the absence of any hydrogen bonding. The weighted average IR spectrum of monohydrated OCS^- (Fig. 4d) shows the dominance of A1 and A2 structures in the ratio of 60 and 28%. The weighted average spectrum for the OH stretching region has two intense peaks at 3520 and 3407 cm^{-1} . The experimental IR spectrum measured by Johnson and coworkers in the OH stretching frequency region of monohydrated OCS^- exhibits two peaks at 3486 cm^{-1} (symmetric stretching frequency) and 3550 cm^{-1} (asymmetric stretching frequency), respectively. The intensity of the symmetric stretching frequency is approximately three times higher than the asymmetric stretching frequency.^[20] The experimental spectral feature of the OH stretching frequency of the monohydrate OCS^- is qualitatively close to the calculated spectral feature of the most stable structure A1 (Fig. 4c). The band position for the calculated IR spectrum in this study is at the higher side as compared with the experimental value, which was also observed in their calculation performed at the B3LYP level of theory. The CO stretching frequency of the OCS^- is close to the water bending region and hence, there is congestion in that region of the IR spectrum. The spectral features at 1556 and 1586 cm^{-1} in the weighted average spectrum belong to the CO stretching of OCS^- core in the monohydrated environment, whereas feature at 1610 cm^{-1} belongs to the water bending region. The peaks between 700 and 800 cm^{-1} belong to the CS stretching frequency of OCS^- core in the monohydrated cluster and the spectral feature around 500–600 cm^{-1} belongs to the OCS bending and wagging of hydrogen atoms of water molecule. Structure A1 shows the red shift in CO stretching and blue shift in CS stretching, whereas opposite trend has been found for structure A2. The shift in CO and CS stretching modes of OCS^-

depends on the manner in which water is hydrogen bonded to OCS^- .

The IR spectrum of most stable and the weighted average IR spectrum of dihydrated OCS^- have been depicted in Figures 4e and 4f. Dihydrated clusters of OCS^- consist of IHB between the water molecules along with the SHB and DHB with OCS^- moiety. The frequency of the IHB water molecules depends on their three dimensional arrangement. For example, the IHB in B1 is out of plane and frequency is 3624 cm^{-1} (Fig. 4e), whereas for B2, IHB is in plane and frequency for this arrangement is 3400 cm^{-1} . The maximum red shifted IR band in the O—H stretching region is observed at 3282 cm^{-1} which corresponds to water molecule which has one SHB with sulfur terminal of OCS^- and other OH mode is free. The SHB O—H stretching mode of second water is observed at $\sim 3400 \text{ cm}^{-1}$, whereas the DHB O—H stretching mode of second water is observed in the range of 3525–3650 cm^{-1} . The OH stretching frequency shift for the first water of dihydrated clusters is higher in general as compared with the monohydrated ones which shows the cooperativity of hydrogen bonding. The spectral feature in the range of the 1620–1670 cm^{-1} belongs to the water bending of dihydrated clusters which is blue shifted compared with the water monomer. However, addition of water does not change water bending frequency significantly as compared with the monohydrated clusters and only broadening of the band takes place because of the presence of many conformers. The spectral features around 1500–1580 cm^{-1} and 700–800 cm^{-1} correspond to the CO and CS stretching of the OCS^- core in dihydrated clusters.

The stable structures for the $\text{OCS}^-(3\text{H}_2\text{O})$ cluster have three IHB water molecules of which, either all three or at least two IHB hydrogen-bonded water are interacting with the OCS^- moiety in SHB or DHB fashion. The weighted average IR spectrum of the $\text{OCS}^-(3\text{H}_2\text{O})$ cluster (Fig. 4h) shows many

overlapping bands in the range of 3300–3700 cm^{-1} due to the presence of many different hydrogen-bonded conformers. The weighted average IR spectrum as well as the IR spectrum for the most stable structure of $\text{OCS}^-(\text{H}_2\text{O})_n$ ($n = 4-6$) shows many overlapping bands in the range of 3300–3700 cm^{-1} , and the number of such overlapping bands increases with increase in the number of water molecules as depicted in Figures 4i–4n. Normal mode analysis reveals that OH stretching modes of water are very strongly coupled with each other and their coupling increases with increase in the number of water molecules.

To understand the effect of hydration on the OCS^- moiety, scaled CO and CS stretching frequency along with OCS bending frequency of OCS^- have been calculated for the most stable structure of $\text{OCS}^-(\text{H}_2\text{O})_n$ at the MP2/6-311++G(d, p) level of theory and the values are depicted in Table 4. The CO stretching frequency of the OCS^- moiety in the most stable structure of $\text{OCS}^-(\text{H}_2\text{O})_n$ clusters gets red shifted as compared with the CO stretching frequency of the bare OCS^- , whereas CS stretching frequency gets blue shifted. The effect of hydration on the OCS^- moiety has been further explored by the calculation of the charge on the each atom of the hydrated OCS^- calculated at the MP2/6-311++G(d, p) level of theory (Table 4). The negative charge on the oxygen of OCS^- in the $\text{OCS}^-(\text{H}_2\text{O})_n$ clusters increases, while, it decreases on the sulfur. The trend of change in charge on CO and CS molecule of OCS^- moiety indicates that negative charge is moved toward oxygen from sulfur atom on hydration. Other important observation is that the sum of negative charge on the OCS^- moiety is negative even after the hydration up to six water molecules which indicates that the excess electron is intact with OCS^- moiety and hydration only moves the negative charge toward the oxygen from sulfur. The OCS bending frequency of the OCS^- moiety changes significantly for monohydrated cluster and become constant for higher hydrated clusters. The significant change in OCS bending for monohydrated cluster could be due to direct in-plane DHB of first water molecule to OCS^- moiety.

Conclusions

A systematic *ab initio* study of the structure, vibrational frequency, and energetics of $\text{OCS}^-(\text{H}_2\text{O})_n$ [$n = 1-6$] have been performed to have an in depth understanding of the hydration induced stabilization phenomenon of OCS^- . For small water clusters, water binds with OCS^- by $\text{O}-\text{H}\cdots\text{S}$ and $\text{O}-\text{H}\cdots\text{O}$ hydrogen bonding. It is found that maximum two water molecules can directly bind with OCS^- in DHB arrangement. Most of the minimum energy configurations in $\text{OCS}^-(\text{H}_2\text{O})_n$ cluster show surface structure in which the OCS^- resides at the surface of the water network. In some structures of large water clusters, OCS^- resides in the interior of the water network and their stabilization energy is less. The stability of the particular complex depends on the balance between the IHB of water molecules as well as its interaction with the OCS^- . Weighted average solvent stabilization energy increases with the addition of water molecules, whereas weighted average interaction


energy gets saturated after four water molecules. Weighted average solvent stabilization energy values depict that each water molecule stabilizes the OCS^- by 12.7 kcal/mol which show that addition of successive water molecules lower the energy of OCS^- relative to its neutral state, and hence, provides stability to hydrated clusters. The CO stretching frequency of OCS^- gets red shifted, whereas CS stretching frequency gets blue shifted on hydration. Charge analysis on hydrated clusters of OCS^- indicates that hydration moves the negative charge away from sulfur to oxygen atom of OCS^- .

Acknowledgments

The Authors thank Dr. S. Bhattacharya and Abha Bhattacharya for an impactful reading of the manuscript and providing valuable suggestions.

Keywords: carbonyl sulfide • microhydration • stabilization energy • Gaussian • atmospheric

How to cite this article: S., Mondal, A., Uday Teja, P., Chandra Singh *Int. J. Quantum Chem.* **2015**, *115*, 785–795. DOI: 10.1002/qua.24902

 Additional Supporting Information may be found in the online version of this article.

- [1] S. Gopalakrishnan, D. Liu, H. C. Allen, M. Kuo, M. J. Shultz, *Chem. Rev.* **2006**, *106*, 1155.
- [2] P. Lo Nostro, B. W. Ninham, *Chem. Rev.* **2012**, *112*, 2286.
- [3] B. J. Knurr, C. L. Adams, J. M. Weber, *J. Chem. Phys.* **2012**, *137*, 104303.
- [4] M. Saeki, T. Tsukuda, S. Iwata, T. Nagata, *J. Chem. Phys.* **1999**, *111*, 6333.
- [5] J. C. Marcum, J. M. Weber, *J. Phys. Chem. A* **2010**, *114*, 8933.
- [6] W. H. Robertson, E. G. Diken, E. A. Price, J.-W. Shin, M. A. Johnson, *Science* **2003**, *299*, 1367.
- [7] K. R. Asmis, D. M. Neumark, *Acc. Chem. Res.* **2011**, *45*, 43.
- [8] J. Simons, K. D. Jordan, *Chem. Rev.* **1987**, *87*, 535.
- [9] X.-B. Wang, L.-S. Wang, *Annu. Rev. Phys. Chem.* **2009**, *60*, 105.
- [10] A. K. Pathak, D. K. Maity, *J. Phys. Chem. A* **2009**, *113*, 13443.
- [11] H. M. Lee, D. Kim, K. S. Kim, *J. Chem. Phys.* **2002**, *116*, 5509.
- [12] S. J. Vaughn, E. V. Akhmatkaya, M. A. Vincent, A. J. Masters, I. H. Hillier, *J. Chem. Phys.* **1999**, *110*, 4338.
- [13] P. Ayotte, C. G. Bailey, G. H. Weddle, M. A. Johnson, *J. Phys. Chem. A* **1998**, *102*, 3067.
- [14] P. Ayotte, G. H. Weddle, J. Kim, M. A. Johnson, *J. Am. Chem. Soc.* **1998**, *120*, 12361.
- [15] S. A. Corcelli, J. A. Kelley, J. C. Tully, M. A. Johnson, *J. Phys. Chem. A* **2002**, *106*, 4872.
- [16] J. M. Weber, J. A. Kelley, W. H. Robertson, M. A. Johnson, *J. Chem. Phys.* **2001**, *114*, 2698.
- [17] T. I. Yacovitch, N. Heine, C. Brieger, T. Wende, C. Hock, D. M. Neumark, K. R. Asmis, *J. Phys. Chem. A* **2013**, *117*, 7081.
- [18] J. Zhou, G. Santambrogio, M. Brümmer, D. T. Moore, L. Wöste, G. Meijer, D. M. Neumark, K. R. Asmis, *J. Chem. Phys.* **2006**, *125*, 111102.
- [19] Y. Miller, G. M. Chaban, J. Zhou, K. R. Asmis, D. M. Neumark, R. Benny Gerber, *J. Chem. Phys.* **2007**, *127*, 094305.
- [20] W. H. Robertson, E. A. Price, J. M. Weber, J.-W. Shin, G. H. Weddle, M. A. Johnson, *J. Phys. Chem. A* **2003**, *107*, 6527.
- [21] E. Garand, T. Wende, D. J. Goebbert, R. Bergmann, G. Meijer, D. M. Neumark, K. R. Asmis, *J. Am. Chem. Soc.* **2009**, *132*, 849.
- [22] D. J. Goebbert, E. Garand, T. Wende, R. Bergmann, G. Meijer, K. R. Asmis, D. M. Neumark, *J. Phys. Chem. A* **2009**, *113*, 7584.

- [23] L. Jiang, S.-T. Sun, N. Heine, J.-W. Liu, T. I. Yacovitch, T. Wende, Z.-F. Liu, D. M. Neumark, K. R. Asmis, *Phys. Chem. Chem. Phys.* **2014**, *16*, 1314.
- [24] H. Motegi, T. Takayanagi, T. Tsuneda, K. Yagi, R. Nakanishi, T. Nagata, *J. Phys. Chem. A* **2010**, *114*, 8939.
- [25] A. K. Pathak, T. Mukherjee, D. K. Maity, *J. Phys. Chem. A* **2008**, *112*, 3399.
- [26] H. Schneider, K. M. Vogelhuber, J. M. Weber, *J. Chem. Phys.* **2007**, *127*, 114311.
- [27] H. Schneider, J. M. Weber, *J. Chem. Phys.* **2007**, *127*, 174302.
- [28] T. Tsukuda, M. Saeki, R. Kimura, T. Nagata, *J. Chem. Phys.* **1999**, *110*, 7846.
- [29] T. I. Yacovitch, T. Wende, L. Jiang, N. Heine, G. Meijer, D. M. Neumark, K. R. Asmis, *J. Phys. Chem. Lett.* **2011**, *2*, 2135.
- [30] R. J. Ferm, *Chem. Rev.* **1957**, *57*, 621.
- [31] P. D. N. Svoronos, T. J. Bruno, *Ind. Eng. Chem. Res.* **2002**, *41*, 5321.
- [32] L. T. N. Dang, W. C. Stolte, G. Öhrwall, M. M. Sant'Anna, I. Dominguez-Lopez, A. S. Schlachter, D. W. Lindle, *Chem. Phys.* **2003**, *289*, 45.
- [33] G. L. Gutsev, R. J. Bartlett, R. N. Compton, *J. Chem. Phys.* **1998**, *108*, 6756.
- [34] A. Sanov, S. Nandi, K. D. Jordan, W. C. Lineberger, *J. Chem. Phys.* **1998**, *109*, 1264.
- [35] E. Surber, S. P. Ananthavel, A. Sanov, *J. Chem. Phys.* **2002**, *116*, 1920.
- [36] E. Surber, A. Sanov, *J. Chem. Phys.* **2002**, *116*, 5921.
- [37] E. Surber, A. Sanov, *J. Chem. Phys.* **2003**, *118*, 9192.
- [38] M. J. Frisch, G. W. Trucks, H. B. Schlegel, G. E. Scuseria, M. A. Robb, J. R. Cheeseman, G. Scalmani, V. Barone, B. Mennucci, G. A. Petersson, H. Nakatsuji, M. Caricato, X. Li, H. P. Hratchian, A. F. Izmaylov, J. Bloino, G. Zheng, J. L. Sonnenberg, M. Hada, M. Ehara, K. Toyota, R. Fukuda, J. Hasegawa, M. Ishida, T. Nakajima, Y. Honda, O. Kitao, H. Nakai, T. Vreven, J. A. Montgomery, Jr., J. E. Peralta, F. Ogliaro, M. Bearpark, J. J. Heyd, E. Brothers, K. N. Kudin, V. N. Staroverov, R. Kobayashi, J. Normand, K. Raghavachari, A. Rendell, J. C. Burant, S. S. Iyengar, J. Tomasi, M. Cossi, N. Rega, J. M. Millam, M. Klene, J. E. Knox, J. B. Cross, V. Bakken, C. Adamo, J. Jaramillo, R. Gomperts, R. E. Stratmann, O. Yazyev, A. J. Austin, R. Cammi, C. Pomelli, J. W. Ochterski, R. L. Martin, K. Morokuma, V. G. Zakrzewski, G. A. Voth, P. Salvador, J. J. Dannenberg, S. Dapprich, A. D. Daniels, Ö. Farkas, J. B. Foresman, J. V. Ortiz, J. Cioslowski, and D. J. Fox, Gaussian 09 Revision B.01, Gaussian: Wallingford, CT, **2010**.
- [39] G. M. Hartt, G. C. Shields, K. N. Kirschner, *J. Phys. Chem. A* **2008**, *112*, 4490.
- [40] S. S. Xantheas, T. H. Dunning, *J. Chem. Phys.* **1993**, *98*, 8037.
- [41] A. K. Pathak, T. Mukherjee, D. K. Maity, *J. Chem. Phys.* **2006**, *125*, 074309.
- [42] A. K. Pathak, T. Mukherjee, D. K. Maity, *J. Chem. Phys.* **2007**, *126*, 034301.
- [43] G. C. Pimental, A. L. McClellan, The hydrogen bond. A Series of Chemistry Books, W.H. Freeman and Company, San Francisco and London, **1960**.
- [44] M. Falk, *Spectrochim. Acta A* **1984**, *40*, 43.

Received: 23 December 2014
Revised: 17 February 2015
Accepted: 23 February 2015
Published online 13 March 2015